LAWRENCE
LIVERMORE
NATIONAL
LABORATORY

UCRL-CONF-214910

Laser-Plasma Interactions in High-Energy Density Plasmas

C. G. Constantin, H. A. Baldis, M. B. Schneider, D. E. Hinkel, A. B. Langdon, W. Seka, R. Bahr, S. Depierreaux

August 30, 2005

Inertial Fusion Science and Applications
Biarritz, France
September 4, 2005 through September 9, 2005

Disclaimer

This document was prepared as an account of work sponsored by an agency of the United States Government. Neither the United States Government nor the University of California nor any of their employees, makes any warranty, express or implied, or assumes any legal liability or responsibility for the accuracy, completeness, or usefulness of any information, apparatus, product, or process disclosed, or represents that its use would not infringe privately owned rights. Reference herein to any specific commercial product, process, or service by trade name, trademark, manufacturer, or otherwise, does not necessarily constitute or imply its endorsement, recommendation, or favoring by the United States Government or the University of California. The views and opinions of authors expressed herein do not necessarily state or reflect those of the United States Government or the University of California, and shall not be used for advertising or product endorsement purposes.

UCRL-CONF-214910

The headers will be insert by the Publisher
The headers will be insert by the Publisher
The headers will be insert by the Publisher

Laser-Plasma Interactions in High-Energy Density Plasmas

C.G. Constantin[1], H.A. Baldis[1,2], M.B. Schneider[2], D.E. Hinkel[2], A.B. Langdon[2], W. Seka[3], R. Bahr[3], and S. Depierreux[4]

[1]*University of California at Davis, One Shields Avenue, Davis, CA 95616, USA*
[2]*Lawrence Livermore National Laboratory, 7000 East Avenue, Livermore, CA 94550*
[3]*Laboratory for Laser Energetics, 250 East River Road, Rochester, NY 14623-1299, USA*
[4]*Departement de Conception et de Realisation des Experimentations, CEA-DIF, France*

Abstract. Laser-plasma interactions (LPI) have been studied experimentally in high-temperature, high-energy density plasmas. The studies have been performed using the Omega laser at the Laboratory for Laser Energetics (LLE), Rochester, NY. Up to 10 TW of power was incident upon reduced-scale hohlraums, distributed in three laser beam cones. The hot hohlraums fill quickly with plasma. Late in the laser pulse, most of the laser energy is deposited at the laser entrance hole, where most of the LPI takes place. Due to the high electron temperature, the stimulated Raman scattering (SRS) spectrum extends well beyond $\omega_0/2$, due to the Bohm-Gross shift. This high-temperature, high-energy density regime provides a unique opportunity to study LPI beyond inertial confinement fusion (ICF) conditions.

1. INTRODUCTION

Novel plasma conditions are created by shining a powerful laser beam onto the high-Z walls enclosing a cavity (hohlraum) [1], which is sufficiently reduced in size to allow high electron temperatures to be reached. These platforms are also useful as high-temperature radiation sources for material science studies of matter driven to extreme conditions. The optimization of the laser energy coupling to the hot hohlraums [2], critical for improving their efficiency as radiation sources, implies knowledge and control over the loss mechanisms. These are mainly stimulated backscattering (Raman and Brillouin) of the laser light [3], along with laser beam instabilities such as filamentation, spraying, deflection, and cross-beam energy transfer [4]. The small targets fill with plasma, so the laser deposition region moves towards the laser entrance hole. This small region becomes very hot. The results we report show the time history of the stimulated Raman scattering (SRS), which shows signs of hohlraum filling. The information carried by the scattered light is related to the plasma density, and through the Bohm-Gross shift in the dispersion relation [5] to the electron temperature. We will also show the dependence of the backscattering reflectivity and spectra features on the target size.

2. EXPERIMENTAL CONFIGURATION

The targets used in these experiments are empty half hohlraums with a back wall. The hohlraums have 25 μm thick gold walls. Three different size targets were used in order to observe the scaling of

the laser energy coupling to the target. Thus, the smallest target diameter is 600 μm with a length of 660 μm, and the largest diameter is 1600 μm with 1760 μm length (see Table 1). The laser entrance hole (LEH) is equal to the hohlraum's diameter.
The experiments were performed at the OMEGA laser [6], at LLE. Nineteen laser beams at ~ 500 J/beam, in 1 ns pulses and 351 nm ($3\omega_0$) wavelength illuminated the target from one side, aimed and focused at the center of the LEH. The beams are grouped in three cone angles around the target axis: 21.4° for the inner cone of beams (cone 1, with 4 beams), 42° for the center cone (cone 2, with 5 beams), and 58.8º for the outer beams (cone 3, with 10 beams). The beams expand with f/6.7 and the nominal beam spot size is 80 μm.

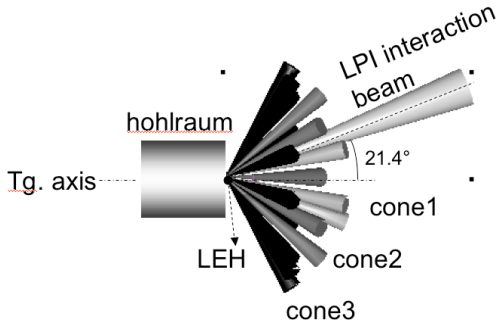

Figure 1. A typical Au hohlraum with back wall, irradiated by the Omega laser beams incident on the LEH under 21.4º, 42º, and 58.8º (cone 1- light grey, cone 2- dark grey, and cone 3- black, respectively). The interaction beam for backscattering measurements (LPI interaction beam) belongs to cone 1.

The beams in cone 1 and 2 are smoothed with distributed polarization rotators (DPR), which split the beams into two beams of opposite polarization separated by ~80μm. This reduces the intensity of the hot spots to some degree. The outer beams with steeper incidence angles (in cone 3) are not smoothed.
For the laser light backscatter measurements a full aperture backscattering diagnostic (FABS) is used, consisting of a system of calorimeters and spectrometers plus streak cameras. The calorimeters measure the time-integrated Raman (SRS) and Brillouin (SBS) backscattered light, while the streak camera-spectrometer system resolves spectrally and temporally the SRS and SBS signals. The SRS scattered light is fed into a 1/3 m Czerny-Turner spectrometer by optical fibers that collect the signal from the lens of the interaction beam shown in Fig. 1, which, in this experiment, is a cone 1 beam.

3. RESULTS

Figure 2 shows time-resolved SRS spectra for the three target types. The wavelength and time axis were calibrated and corrected for the optical fiber dispersion. The 1 ns laser pulse is plotted below the spectrum, together with the interaction beam pulse which had the same shape and duration.

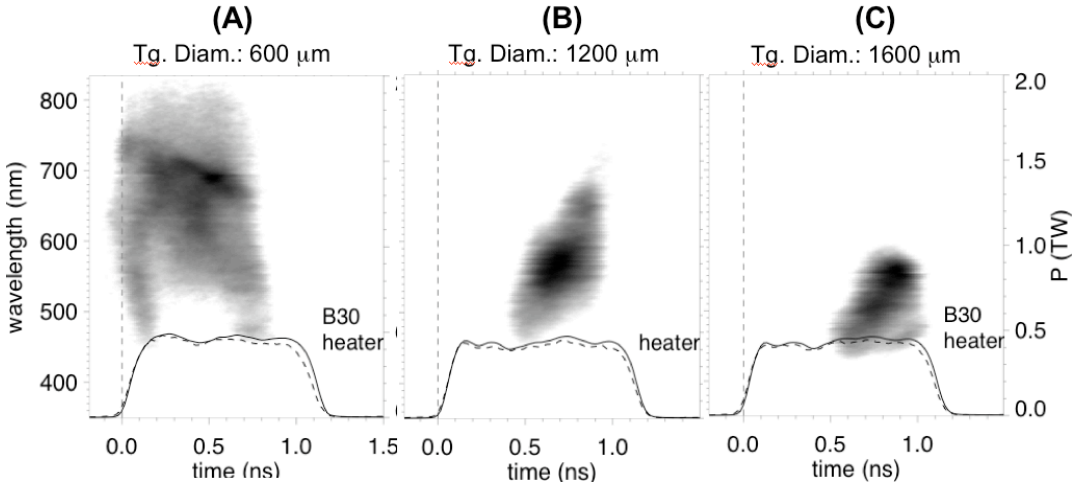

Figure 2. Stimulated Raman scattering spectra detected with time resolution, originating from targets with different size scales: (A) diameter 600 μm, (B) 1200 μm, and (C) 1600 μm. The laser pulse shape (heater) is plotted together with the Raman signal (right-hand side axis). The dotted line represents the interaction beam pulse shape.

The time-history of the SRS spectrum shows wavelength shifts well beyond the typical limit of $2\lambda_0$=702 nm. After reaching the maximum value, the Raman wavelength tends to decrease slowly in time. We associate the early time behavior with plasma filling of the hohlraum to ~$0.25n_{cr}$ where n_{cr} is the critical density. We call the time at which maximum Raman wavelength shift occurs, the 'fill time'. The fill time, maximum Raman wavelength, and absolute Raman energy vary with target size. The results are shown in Table 1.

Raman wavelengths beyond $2\lambda_0$ indicate high electron temperatures due to the Bohm-Gross shift in the dispersion relations:

$$\omega_0 = \omega_{SRS} + \omega_{EPW} \qquad (1)$$

$$\omega_{EPW}^2 = \omega_{pe}^2 + 3k_{EPW}^2 v_{th}^2 \qquad (2)$$

with ω_0 the laser frequency, ω_{SRS} the scattered wave frequency, ω_{EPW} and k_{EPW} the electron plasma wave frequency and wave number, respectively, and $v_{th} = \sqrt{T_e / m_e}$ the thermal velocity of the electrons in a Maxwellian distribution. In Eq. (2), the second term on the right-hand side expresses the temperature dependent Bohm-Gross shift.

In the small target the fill time is short. This target also has the longest Raman wavelength measured, implying the highest plasma temperature. In the larger targets, the Raman wavelength is always increasing, pointing toward a slow, or incomplete plasma fill.

The reflectivity of Raman and Brillouin backscattering is decreased if light is sprayed outside the beam cone. It is also affected by non-direct backscattered light from other beams.

TABLE 1. Summary of the fill time (τ_{FILL}), maximum Raman wavelength (λ_{MAX}), and reflectivity (R%) of the backscattering for each target size probed.

DIAMETER (μm)	LENGTH (μm)	$\tau_{FILL\ (ns)}$	λ_{MAX} (nm)	R_{SRS} (%)	R_{SBS} (%)
600	660	0.2	740	5.4	1.8
1200	1320	0.3	670	5	0.7
1600	1760	0.4	580	2.5	0.8

According to 2D, hydrodynamic numerical simulations (LASNEX) [7] the small targets reach electron densities in the range from $0.1n_{cr}$ to $0.4n_{cr}$ at the LEH, and temperatures between 10 and 18 keV during the time when SRS is observed. To better understand the correlation between data and

simulations, we generated an analytic model based on the dispersion and resonance conditions (Eqs. 1 and 2). In Fig. 3, the measured Raman wavelength is plotted against the ratio between the electron density and the critical density for different temperatures and different $k\lambda_{De}$. For our case we assume $k\lambda_{De}<0.45$ (where λ_{De} is the Debye length of the plasma). The limit for the SRS is reached at $n_e=0.25n_{cr}$ (for $T_e=0$) and lower for temperatures characteristic to our regimes.

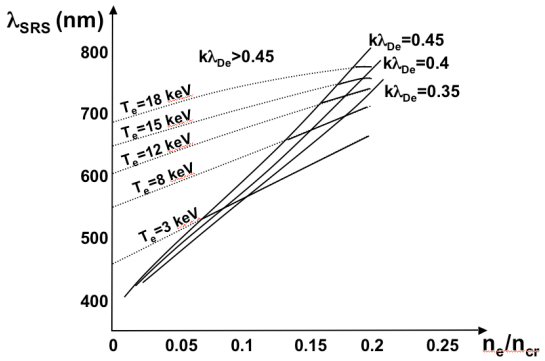

Figure 3. Stimulated Raman scattering wavelength dependence on electron density, for temperatures ranging between 3 and 18 keV. The plot refers to the plasma at the LEH, during the laser beam pulse and it is analytically determined using the dispersion and resonance conditions for SRS.

According to this model, for Raman wavelengths approaching our experimental observations, plasma temperatures as high as 18 keV, at a density around $0.15n_{cr}$ for the small targets, and 8 keV for the largest targets, at similar densities, are reached. These densities, according to numerical simulations, are describing the plasma situation around 300 ns after the laser pulse starts, which is beyond the fill time for the small targets, and therefore at the LEH. For the large targets, such values are most probably reached later in time than in small targets, and the scattering is collected from different locations inside the target, along the interaction beam path.

4. CONCLUSIONS

Stimulated Raman scattering was studied in reduced-scale hohlraums. Targets with small diameters (600 μm) have Raman spectra that extend beyond $2\lambda_0$, which indicates a high electron temperature. Using the SRS dispersion relations, and eliminating regions where SRS gain is low, the SRS spectra can be used as a diagnostic for T_e and n_e.

A comparison between hohlraums with diameters of 600, 1200 and 1600 μm reveals how the Raman spectrum scales with the target size, both in wavelength shift and duration. Thus, for targets with large diameters (Figure 2, (B) and (C)) it appears that the plasma density increases to the SRS lower threshold (when the scattered signal starts to be observed) slower than for the small diameter targets. According to numerical simulations, this lower threshold value is around $0.1n_{cr}$.

This represents a step in a sequence of studies that aim the development of efficient thermal radiation sources from hohlraum targets, irradiated by powerful lasers at OMEGA and NIF levels [8].

Acknowledgments

The authors would like to thank to all contributors to this work, and especially to the LLNL and OMEGA laser crew (LLE) for their invaluable support and effort in making every experiment a success. This work was performed under the auspices of the U.S. Department of Energy by the University of California, Lawrence Livermore National Laboratory under Contract No. W-7405-ENG-48 and grant number DE-FG52-2005NA26017 (NLUF).

References

[1] J.D. Lindl et al., Phys. Plasmas Vol. 11, 339 (2004)
[2] M.B. Schneider et al., in Proceedings of the Fourth International Conference on Inertial Fusion Sciences and Applications, Biaritz, France, 2005 *(to be published)*
[3] W. Kruer, Phys. Plasmas Vol.7, 2270 (2000)
[4] D.E. Hinkel et al., Phys. Plasmas Vol. 12, 056305-1 (2005); D.E. Hinkel et al., in Proceedings of the Third International Conference on Inertial Fusion Sciences and Applications, Monterey, 2003, p. 242
[5] W. Seka et al., Phys. Fluids Vol. 27, 2181 (1984)
[6] T.R. Boehlyet al., Rev. Sci. Instrum. Vol. 66, 508 (1995)
[7] G. Zimmerman, W. Kruer, Comments Plasma Phys. Controlled Fusion Vol. 2, 885 (1975)
[8] D.E. Hinkel et al., in Proceedings of the Fourth International Conference on Inertial Fusion Sciences and Applications, Biaritz, France, 2005 *(to be published)*